IEEE Robotics and Automation Letters (RAL) paper presented at the
2020 IEEE/RSJ International Conference on Intelligent Robots and Systems (IROS)
October 25-29, 2020, Las Vegas, NV, USA (Virtual)

Adaptive Aerial Grasping and Perching with Dual Elasticity Combined Suction Cup

Sensen Liu, Wei Dong, Zhao Ma, and Xinjun Sheng*

***Abstract*— To perch on or grasp the objective surface using the suction cup-based manipulator, the precise contact control is commonly required. Improper contact angle or insufficient contact force may cause failure. To enhance the tolerance to flight control insufficiency, a suction cup that comprises an inner soft cup and an outer firm cup to facilitate its engagement without reducing the adhesion stiffness is investigated. The soft cup is adaptable to the angular error induced by the multicopter and the resulting adhesion force can draw the firm cup and correct the angular error between the firm cup and the surface. These effects increase the engagement rate and reduce the dependence on precise control. The outer firm cup is devoted to providing a large adhesion force and a stiff base for subsequent tasks. To reduce the air evacuation time in the firm cup, a novel self-sealing structure is designed. Based on the combined cup, we build a multifunctional aerial manipulation system which can execute perching or lateral aerial grasping tasks. With the proposed prototype, the comparative flight experiments involving perching on a wall under disturbance and grasping an object are conducted. The results demonstrate that our proposed suction cup outperforms the conventional cup.**

I. Introduction

Perching and aerial grasping are becoming a promising research field with the development of aerial manipulation. Many researchers have proposed various schemes to endow unmanned aerial vehicles (UAVs) with the capability of manipulation such as inspection and maintenance [1]–[3], transportation [4], [5], grasping and manipulation [6], [7]. One common topic in the research is to tackle the limited payload capability and sensitivity to the interaction force of the UAV system. To circumvent the problem, some researchers have proposed a concept of perch-and-manipulate. Tsukagoshi et al. [8] presented a system to perch on the door and twist the knob. In [1], the authors presented a multicopter robot with a top gripper for perching and a bottom arm for precise manipulation. Estrada et al. [9] achieved forceful manipulation with micro air vehicle by perching on a rigid substrate. These perch-and-manipulate applications show the potential requirements for a stable and stiff base provided by perching. Moreover, perching UAVs can save energy by not requiring the main propulsion motors to be running.

Generally speaking, the mechanisms in previous work to achieve perching and aerial grasping can be categorized into three groups: claws [10]–[15], micro-spines ingression or hook [16]–[18], surface attachment [8], [19]–[26]. The characteristics of various perching or aerial grasping strategies have been analyzed thoroughly [27], [28]. Wherein, for the object with a large curvature and relatively smooth non-porous surface, a vacuum suction cup is appropriate, which is also our focus in this paper. To engage the suction cup, a pushing force is required to seal the cup with the object surface. The required force will be much larger when the angular errors between the cup and the surface are significantly induced by the floating platform in the presence of disturbance or multiple cups using one central pump. It is well known that it is also difficult for a multicopter to provide a large lateral force if the grasping direction is horizontal. The resulting reaction force may destroy the stabilization of the drone.

Many schemes have been explored in previous research to facilitate the adherence of the suction cup. The authors in [19], [29], [30] designed various force controllers to regulation the contact force between the suction cup and the object during perching. All of the experiments were conducted indoor without considering the outdoor disturbance factor such as crosswind and also no failure or success ratio was presented and they also did not consider the adaptability to the angular errors. In [8], [31], compliant mechanisms were implemented to accommodate the error of orientation or position induced by the UAVs and thus the force to laterally perch on or vertically grasp the surface could be decreased. However, Tsukagoshi et al. [8] indicated that the soft compliant support decreased the stiffness of the base and even made it difficult to bear the shear force. The authors in [32]–[34] designed a novel self-sealing suction cup and mounted them on a UAV to implement vertical aerial grasping and simulated lateral perching. Although the versatility and weight reduction were achieved by employing multiple cups connecting one central pump, the required contact force to engage the cups was still very large since the cups were unpliable. Therefore, the gravity of the quadrotor had to be exploited to achieve vertical grasping or a uniquely designed propulsion core had to be employed to provide enough lateral force to achieve lateral grasping. The experiment of lateral grasping was only demonstrated on a simulated cart. For a conventional multicopter to achieve lateral perching or grasping, the higher requirements for contact force will increase the difficulty of attaching the suction cup and reduce the success rate, which will be experimentally verified in this article. To summarize, although some existing work has achieved lateral perching and vertical grasping by suction-

This work is partially supported by the Scientific and technical innovation 2030 – "Artificial Intelligence of New Generation" Major Project (2018AAA0102704) and National Natural Science Foundation of China (Grant No. 51975348, 51605282).

The authors are with the State Key Laboratory of Mechanical System and Vibration, Robotics Institute, School of Mechanical and Engineering, Shanghai Jiao Tong University, 800 Dongchuan Road, Shanghai, China. Xinjun Sheng is the corresponding author. xjsheng@sjtu.edu.cn.

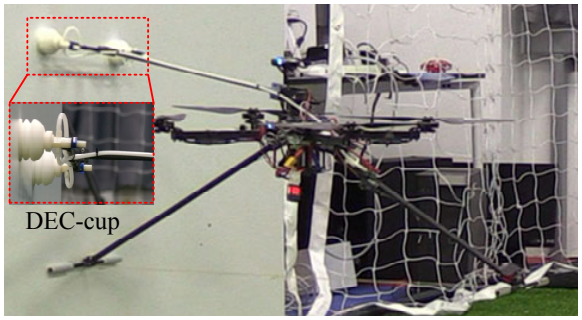

Fig. 1. The aerial manipulation system with a pair of DEC-cups is perching on a wall. The left figure shows the close-up view of DEC-cups.

cups, the large contact force has to be provided via multicopter to compensate the angular errors. No research effort, to the best of our knowledge, has achieved lateral suction cup aerial grasping, which is more sensitive to large contact force that may push the object away. That is, how to increase the adaptability of the suction cup to the angular error as well as guarantee a large adhesion force and the stiffness of perching is still an unanswered question.

To address the problem, we propose an aerial manipulation equipped with our dual elasticity combined suction cup (DEC-cup) as is shown in Fig.1. The gripper consisting of two DEC-cups is configured at the lateral of the quadrotor. The inner soft cup in the DEC-cup has higher adaptability to the angular error induced by the floating of the multicopter. This property of the soft cup reduces the requirement for the contact force and controlling of the multicopter. The outer firm cup can provide a large adhesion force and a stiff base, which will benefit the manipulation after perching.

The contributions of this paper are as follows:

1) Propose a scheme combining a soft cup and a firm cup. The scheme can guarantee the adaptability to the angular error and the large adhesion stiffness, adhesion force.
2) A novel self-sealing firm suction cup is devised to connect the firm cup to the central pump to reduce the air evacuation time.
3) A multifunctional aerial manipulation system that can execute perching on a vertical surface and aerial grasping in the lateral direction is presented based on our combined suction cup.

The structure of the paper is as follows. Section II presents our design and the selection of some key dimensions. Section III describes the performance of the soft cup and the relative length of the soft cup is optimized. In Section IV, the validation of the self-sealing structure of the outer firm cup and the performance verification of the DEC-cup in the perching and aerial grasping tasks were conducted and the corresponding results are discussed. Conclusions are given in Section V.

II. DESIGN AND METHOD

In this section, we present our design in three subsections. In Section II-A, the design of our combined suction cup is depicted and the corresponding working process is illustrated. In Section II-B, the self-sealing structure of the firm cup is detailed and some dimensions are analyzed. In Section II-C, we present the design of the multifunctional aerial manipulation system and analyze the load capability.

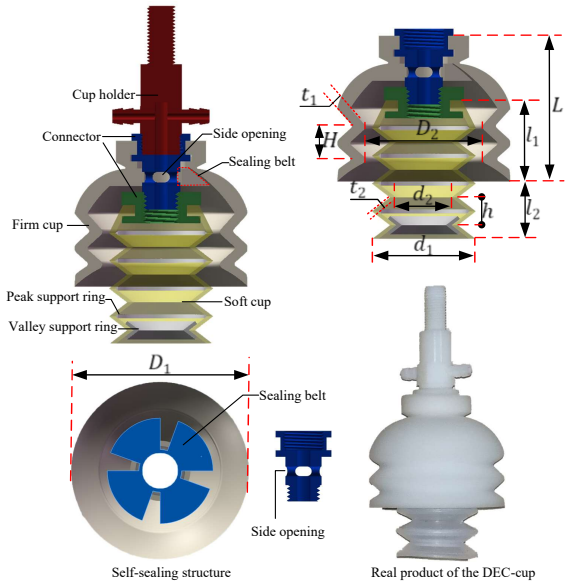

Fig. 2. Overview of the dual elasticity combined suction cup.

TABLE I
MAIN DIMENSION PARAMETERS OF DEC-CUP (mm)

D_1	D_2	d_1	d_2	L	l_1	l_2	t_1	t_2	H	h
50	34	30	16	42	18	22	2.8	1.1	10	8

A. Design of Dual Elasticity Combined Suction Cup

The dual elasticity combined suction cup (DEC-cup) is detailed in Fig.2. The DEC-cup contains an inner soft cup (30 Shore A), an outer firm cup (55 Shore A), a rigid support ring in soft cup, a connector of the firm cup, a connector of the soft cup and a suction-cup holder. The main dimensions are labeled in Fig.2 and the specific parameters are manifested in Table.I. The soft cup is made of silicone rubber by injection molding process and the firm cup is made of Hei-Cast 8400 by vacuum molding. Other rigid parts are made of VeroWhitePlus photosensitive resin by a 3D printer. Fig.2 also demonstrates the inner structure of the outer firm cup and the corresponding connector with side openings. This design realizes the self-sealing functionality which will be elaborated in Section II-B.

The working process of the DEC-cup is shown in Fig.3. There is an initial angular error when the DEC-cup contacts the object surface. Owing to the pliability of the soft material and the bellows structure, the sealing of the soft cup can be finished under a small reaction force and this process is dubbed as the sealing phase. After the sealing phase, the air in the cup can be further evacuated and the adhesion force will generate. This phase is termed as the adhesion phase. If

the engagement process is quasi-static, it can be expressed in following formulas:

$$\tau_g = F_g \times R \tag{1}$$

$$F_e = F_N + F_n - F_g \tag{2}$$

$$F_l = F_G - (F_N + F_n) \tag{3}$$

Where τ_g is the torque induced by F_g around the fulcrum in Fig.3 (b) and F_g is the adhesion force of the soft cup induced by gauge pressure and R is the radius of the firm cup and F_e is the external force exerted on the cup holder and F_N is the force exerted on the firm cup from the surface and F_n is the force exerted on the soft cup from the surface and F_l is the payload force exerted on the cup holder and F_G is the adhesion force of the firm cup. Therein, $F_n \approx 0$ because the inner cup is very soft and l_1 is long enough to avoid the compression of the soft cup.

Equation (1) illustrates that the adhesion force of the soft cup generates a torque to correct the angular error. It is worth noting that the torque τ_g is always in the direction to eliminate the angular error, which will significantly benefit the sealing of the firm cup. Fig.3 (c) shows the phase during which the adhesion of the soft cup and the sealing of the firm cup occur simultaneously. This phase can be described by (2). For a certain minimal F_N to seal the firm cup, F_e can be small even zero if F_g is approximately designed, which means the force to finish the sealing of the firm cup will decrease. Equation (3) describes the adhesion phase of the firm cup and large F_l can be provided by F_G and a stiffer base can also be provided because of the firmness of the outer cup. For the dynamic situation, when the drone impacts the surface at a higher speed, the drone may be rebounded. In this case, the F_g can counteract the resilient momentum and pullback the drone again.

To summarize, the soft cup has better adaptability to the angular misalignment and the adhesion force can generate the torque to correct the angular error of the firm cup relative to the object surface. Furthermore, the adhesion force can also attract the firm cup to the surface. Hence, the soft cup significantly facilitates the sealing of the firm cup. For the firm cup, it is used to provide a larger adhesion force and a stiffer support for payloads. That is our combined cup scheme decouples the sealing phase and the adhesion phase so the strong adaptability and a large adhesion stiffness can be designed independently.

B. Design of the Self-Sealing Structure

During the sealing phase and the adhesion phase of the firm cup, the air between the firm cup and the soft cup cannot be evacuated. Therefore, an air way to the central pump is necessary for the firm cup after the soft cup is closed (Fig.3 (c)). If the firm cup is not used, that air way should be closed to avoid the air leakage during the sealing of the soft cup (Fig.3 (a)). In this article, we design a self-sealing structure to implement this function without any sensing or control and the enlarged view of details is shown in Fig.4. The neck of the firm cup was design to be thiner which makes the torsion

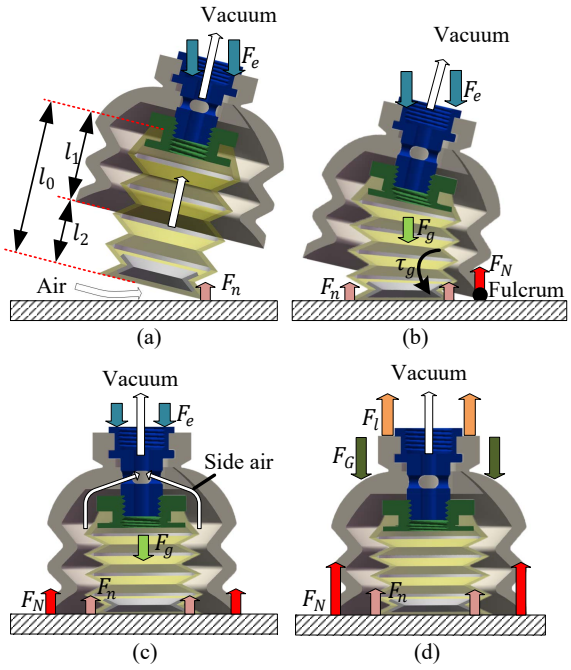

Fig. 3. The working process of the DEC-cup. (a) The initial contact of the DEC-cup. (b) The sealing phase of the soft cup. The fulcrum is the contact point of the firm cup with the surface. The angular error is corrected by the torque τ_g. (c) The adhesion phase of the soft cup and the sealing phase of the firm cup occur at the same time. The side air indicates the air between two cups is evacuated via the opening of the self-sealing structure. (d) The adhesion phase of the DEC-cup.

around the neck easier. Hence, the weaker neck can be regarded as a fulcrum and other parts can be approximately regarded as a rigid body with negligible deformation. When the firm cup is compressed on the surface, the reaction force F_N will generate a torque on the thinner neck. The torque rotates the sealing belt by an angle α. Then the gap δ between the sealing belt and the side opening will emerge and the firm cup can connect the central pump through the gap. The air between the firm cup and the soft cup can be evacuated. We call this state of the self-sealing structure the open state as is shown in the left part of Fig.4. Once the firm cup does not contact the surface, F_N will disappear and the firm cup can recover and the sealing belt will press the side opening to avoid the air leakage. This state of the self-sealing structure is called the closed state as is shown in the right part of Fig.4.

To demonstrate the mechanism of the self-sealing structure, we show the qualitative analysis which is to be verified experimentally. Referring to Fig.4, we suppose that the gap δ determines the opening degree of the self-sealing structure. The gap δ is determined by the rotation angle α of the sealing belt and the distance from the fulcrum to the lower edge of the side opening. The angle α is induced by the torque which is determined by the reaction force F_N and the distance from the action point of the force to the fulcrum. The above analysis can be expressed as the following formulas. First, the torque induced by F_N can be derived from the moment equilibrium equation for the center of the end face of the

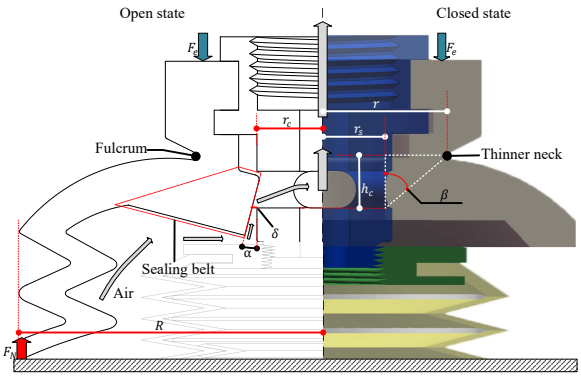

Fig. 4. The comparison of the open state and the closed state of the self-sealing structure. The left part is the open state. In this state, the air way between the firm cup and the central pump is opened by the gap δ. The right part is the closed state. In this state, the gap δ disappears due to the elastic recovery.

firm as

$$\oint_0^{2\pi R} R\frac{F_N}{2\pi R}dx = T + \oint_0^{2\pi r} r\frac{F_N}{2\pi r}dx \tag{4}$$

$$T = k\alpha. \tag{5}$$

Where r is the radius of the thinner neck and T is the torque counteracting the torsional moment induced by F_N, which is also the torque to rotate the sealing belt. k is the equivalent coefficient of stiffness considering the effect of the whole structure and material, to map torque T and the torsional angle α around the fulcrum at the neck. Then the gap δ at the lower edge of the side opening of the connector can approximately be:

$$\begin{aligned}\delta &\approx \alpha\sqrt{(r-r_s)^2+h_c^2}\cos\beta - \\ &\alpha\sqrt{(r-r_s)^2+h_c^2}\sin\beta\tan\alpha - (r_c - r_s) \\ &\approx \alpha h_c - (r_c - r_s).\end{aligned} \tag{6}$$

Where r_s is the radius of sealing belt and h_c is the vertical distance of the fulcrum and the lower edge of the side opening and $\beta = \arctan((r-r_s)/h_c)$ and r_c is the inner radius of connector. All these notations are illustrated in Fig.4. We assume the angle α is small and then we get the relationship between F_N and δ from (4) to (6):

$$F_N \approx \frac{(\delta + r_c - r_s)k}{(R-r)h_c}. \tag{7}$$

In (7), the r_c, r_s, R, r, h_c are known from the design parameters. The parameter k can be identified when the reaction force F_N and the gap δ are measured by the experiment, which will be done in the future. For a given δ to open the self-sealing structure, F_N will decrease if r, k, r_c decrease or R, h_c and r_s increase according to (7). Therein, R, r, r_s and k are related to the design of the firm cup and r_c or h_c is only determined by the connector. Hence, the activation threshold to open the self-sealing structure can be regulated independently after the manufacture of the firm cup. Comparing with the self-sealing in [32]–[35], our design comprises only two parts: the firm cup and the corresponding connector so the manufacture and regulation are simplified.

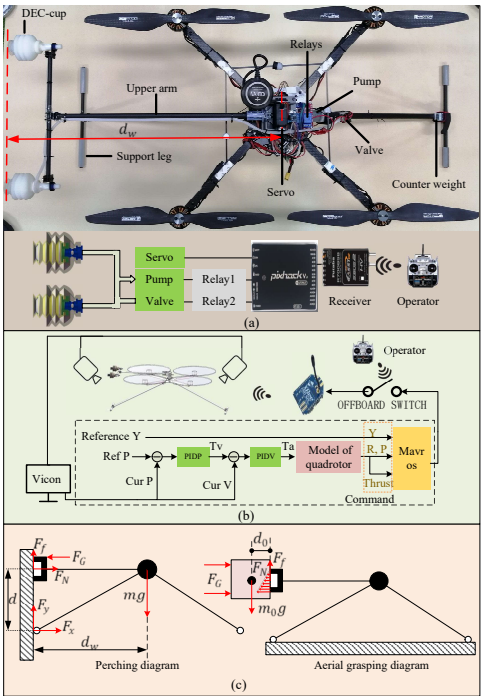

Fig. 5. The framework of the aerial manipulation system and the controller. (a) The structure of the system and the pneumatic system. (b) The cascade PID controller under the Vicon motion capture system. Ref P, Cur P, PIDP, PIDV, Tv, Ta and Y, R, P denotes reference position, Current position from Vicon system, PID parameters in position loop, PID in velocity loop, target velocity, target acceleration, yaw, roll and pitch attitude command respectively (c) The force schema of perching and aerial grasping.

C. Design of Multifunctional Aerial Manipulation System

In order to execute the perching and aerial grasping task, we design a multifunctional manipulation system equipped with the DEC-cup, which is shown in Fig.5 (a). The main structure of the multifunctional system contains an upper arm, the fuselage and a support gear. The upper arm is driven by a top servo and the support gear can be used as the landing gear or the lateral support in perching task as shown in Fig.1. The electronic control system, pneumatic system and the control framework is shown in Fig.5 (a) and (b). The autopilot is based on the PX4 and the controller is based on the cascade PID under the Vicon motion capture system.

Our design aims at perch-and-manipulate task so the payload that the suction cup can provide should be calculated. The force schema of perching and aerial grasping is shown in Fig.5 (c). In Fig.5 (c), the constraint at the lower support point can be regarded as point contact so there is no moment at the support point. Otherwise, a silicone tube is attached on the support beam and we assume the friction coefficient μ between the support point and the wall is the same with that between the silicone cup and the wall. The successful

perching can be depicted as following equations:

$$F_G = \pi R^2 P_G \tag{8}$$

$$nF_G d \geq Smgd_w \tag{9}$$

$$\mu n F_G \geq Smg. \tag{10}$$

Where P_G is the gauge pressure in of the firm cup and n is the number of the cup (all the cups are arranged in horizontal line) and d is the vertical distance between the suction cup and the support point and S is the safety coefficient and m is the mass of the system and g is the gravitational acceleration and d_w is the distance between mass center of the system and the wall.From (8) to (10), we can get:

$$m \leq \frac{n\pi R^2 P_G}{Sg} \cdot \min\{\frac{d}{d_w}, \mu\}. \tag{11}$$

In our design, $n = 2, S = 2, R = 0.025m, P_G = 60kPa, g = 10m/s^2, d = 0.272m, d_w = 0.486m, \mu = 0.6$, and then we get $m \leq 6.59Kg$. The weight of our multicopter system is $1.77Kg$, which is in the payload capacity.

For the aerial grasping in the lateral direction, we assume it is a quasi-static process. The object will produce a torque on the end of the cup so the analysis is as following:

$$\mu n F_G \geq Sm_0 g \tag{12}$$

$$nT_c \geq Sm_0 g d_0 \tag{13}$$

$$T_c = F_G R. \tag{14}$$

Where m_o is the mass of the object and T_c is the critical torque that F_G can generates for the cup with a radius R, which is the maximal torque the cup can provide without disengagement and d_o is the distance between the center of the mass of the object and the end of the cup. Equation (14) is derived from the literature [36]. Therefore, we can obtain the payload capacity as following:

$$m_0 \leq \frac{n\pi R^2 P_G}{Sg} \cdot \min\{\frac{R}{d_0}, \mu\}. \tag{15}$$

From (15), we can know that if $d_0 \leq R/\mu$, the capability of the cup is determined by the friction coefficient.

III. PERFORMANCE AND OPTIMIZATION OF THE SOFT CUP

In this section, we test the performance of the soft cup and optimize its relative length to facilitate the engagement of the firm cup aided by the soft cup. According to (2), if F_g is large enough, the required F_e can be decreased and even rendered unnecessary. Therefore, we select the F_g during the sealing phase of the firm cup as the optimization objective to maximize the contribution of the soft cup for the sealing of the firm cup.

Fig.2 demonstrates the main dimensions of the DEC-cup. Therein, D_1 is determined by the payload capability. For other dimensions like D_2, H, L, d_1, d_2, h, they all influence the performance of the soft and firm cup. However, the design and optimization of the suction cup itself are not within the scope of this article. During the sealing phase of the firm cup, the soft cup will be compressed by air pressure. For a given soft cup, the adhesion force F_g is determined by the gauge pressure and the compressive length. The compressive length refers to the amount of compression relative to the original length of the soft cup as is shown in the bottom of Fig.6 (a). Referring to Fig.3 (a) and (c), the compressive length of the soft cup is equal to l_2 because the deformation of the firm cup is negligible during its sealing phase. Therefore, we dub l_2 as the compressive length which is also the length of the soft cup outside the firm cup and l_1 is the length of the soft cup contained in the firm cup. When given a constant original length of the soft cup l_0, the relationship between l_1 and l_2 is formulated by:

$$l_1 + l_2 = l_0 = 40mm. \tag{16}$$

In practice, we can change l_2 by regulating the position of the soft cup relative to the firm cup in the axial direction. Therefore, the optimization problem can be formulated as follows:

$$\max_{l_2} F_g(l_2). \tag{17}$$

In order to get the largest F_g, we conducted the tensile test of the soft cup to know the relationship between the compressive length l_2 and pull force of the soft cup F_g under the different gauge pressure.The test platform is shown in Fig.6 (a). The main framework is a hand-cranked lifting platform comprising a sliding platform and a support frame. The digital manometer (XZBELEC-AZ82100), the laser ranger (Dongmei-JDC-60) and the dynamometer (AIGU-ZP-100) are mounted on the sliding platform. A soft cup with a holder is connected to the dynamometer and a small plywood board as the object surface is fixed on the support frame beneath the soft cup. A vacuum pump (SC3710PM) with the greatest vacuum degree $60kPa$, a battery and a throttle valve are mounted on the top of the frame. We adjust the height of the soft cup downward with an interval of $2mm$. During a new height, we regulated the throttle valve to control the gauge pressure from $0kPa-60kPa$ with an interval of $5kPa$ for the soft cup with support rings ($2kPa$ for the soft cup without support ring) and the corresponding pull force, the distance data and the gauge pressure were recorded.

Fig.6 (b) and (c) show the results for the soft cup with and without support rings respectively. The contours with different color present different gauge pressure. From Fig.6 (b) and (c), we can know that F_g will increase if the compressive length decreases or the gauge pressure increases. It is worth noting that the maximal gauge pressure and the minimal compressive length cannot be attained at the same time. One reason is that the buckling will occur when soft cup is under a larger gauge pressure and a longer length as is shown in the buckling area in Fig.6 (b) and (c). Another reason is the unavoidable air leakage will reduce the maximal vacuum degree. Fig.6 (b) and (c) indicate that F_g can get the largest value without buckling when the compressive length is $22mm$. Hence, the optimal l_2 is $22mm$. Comparing Fig.6 (b) with Fig.6 (c), we can know that the buckling area of the soft cup with support rings is significantly smaller than that without support ring and the maximal $F_g = 16.78N$ which

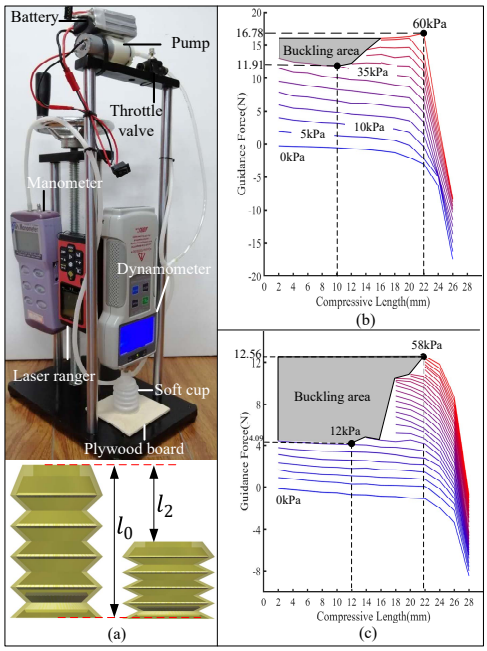

Fig. 6. The test platform and the results of tensile test of the soft cup. (a) The test platform and illustration of the compressive length. The results of the soft cup with support rings. (c) The results of the soft cup without the support ring.

is larger than the activation force of our self-sealing firm cup. These indicate that the rigid supports are very helpful.

IV. EXPERIMENTS

This section presents several tests and experiments to verify the performance of our design. In Section IV-A, the self-sealing design is validated. In Section IV-B the comparative experiments of perching indoor under crosswind or not are demonstrated. In Section IV-C, the comparative experiments of aerial grasping are shown to verify the effectiveness of our design. The discussions are given in Section IV-D.

A. Validation Experiment of the Self-Sealing Structure

In order to verify the validity of our self-sealing design, we conducted a comparative experiment. The test rig is similar with that in Fig.6 (a). In order to measure the air pressure in the space between the soft cup and the firm cup, we designed a bottom board with a measuring hole located in the annulus between the end circle of the soft cup and the firm cup. There is an air tube adapter under the hole and an air pressure sensor (RSCM17100KN090) with the response time $2ms$ connecting to the adapter. As the DEC-cup moved down onto the board, the board will be lifted by the soft cup to compress on the end of the firm cup and the firm cup can be activated by F_g. The air pressure data were recorded at the frequency of $250Hz$. For the comparative group, the only difference is that we employed a connector of the firm cup without the siding openings. We conducted five trials for each group respectively and plot the results as shown in Fig.7.

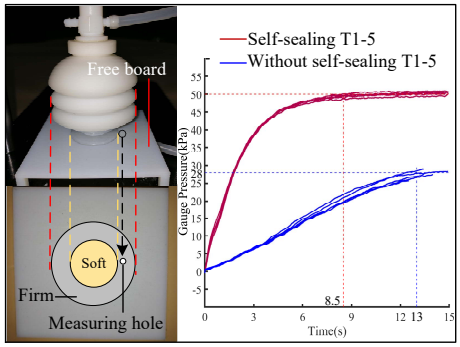

Fig. 7. The test platform with a measuring hole and the results of the gauge pressure over time.

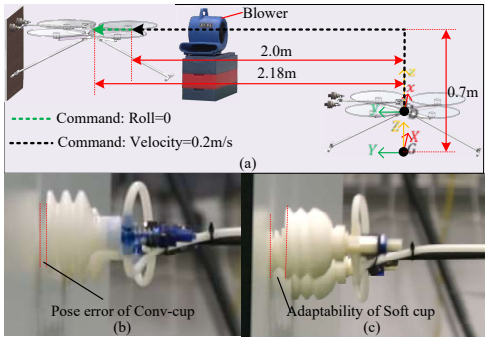

Fig. 8. The comparative experiments of perching. (a) The trajectory and control command of perching. b is the body-fixed frame and G is the ground-fixed frame. (b) The close-up view of the failure of the Conv-cup. (c) The close-up view of the adaptability of the soft cup in the DEC-cup.

B. Comparative Experiment of Perching

We assembled the DEC-cup and a conventional cup (hereafter abbreviated as Conv-cup) on UAV respectively to compare the performance to perch on a vertical wall. The Conv-cup has three bellows made of silicone rubber (55.7 Shore A) and the radius is $25mm$ and the thickness is $2mm$ as is shown in Fig.8 (b). The whole experiment is under the Vicon motion capture system. The prescribed trajectory is in the $z-y$ vertical plane shown in Fig.8 (a). In order to alleviate the influence of the human factor, the process of the perching is autonomous. The operator used the remote control to open the vacuum pump and close the release valve and then switch the quadrotor into the off-board mode. The thrust and attitude command derived from PID controller will be sent to the quadrotor. When the quadrotor is near to the wall, a command roll angle $\Phi = 0$ is used until the perching succeeds. The blower at the side of the wall is used to imitate the crosswind disturbance. In this experiment, the wind speed is $2.5m/s$ at the perching point. We conducted two groups of experiments for the DEC-cup and the Conv-cup respectively. One is in the absence of the crosswind and the other is under the crosswind disturbance. There are ten trials in each group. The results are shown in Table II.

C. Comparative Experiment of Aerial Grasping

The scenario for the aerial grasping is presented in Fig.9 (a). One object is made by sticking a foam board on a LEGO

TABLE II
RESULTS OF COMPARATIVE EXPERIMENTS OF PERCHING AND AERIAL GRASPING

		No crosswind	Crosswind
Perch	DEC-cup	9/10	9/10
	Conv-cup	8/10	2/10
Aerial grasp	DEC-cup	9/10	–
	Conv-cup	0/10	–

– indicates we did not conduct corresponding experiments.
a/b indicates task is completed a times in b times trial.

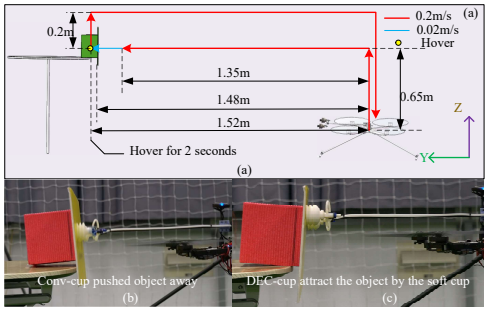

Fig. 9. The comparative experiments of aerial grasping. (a) The trajectory and control command of aerial grasping. (b) The Conv-cups push the object away and failed. (c) The DEC-cups attract the object by soft cup under small reaction force.

box and weighs $132.8g$. The object is put on the edge of a table and an outward offset is for the position error. The trajectory containing three phases are shown in Fig.9 (a). In the fast approaching phase, the quadrotor will reach the point in front of the object surface by $0.13m$. In the slow approaching phase, the quadrotor will keep flying $0.17m$ forward. The two seconds hovering phase is to ensure enough time to finish the engagement. And then the object will be lifted a little and return to the take-off point. We conducted experiments for the DEC-cup and the Conv-cup respectively without disturbance. There are also ten autonomous trials in each experiment. The result is shown in Table II.

D. Discussion

Fig.7 shows the good consistence of five trials in each group. The gauge pressure of the self-sealing cup can rise to $50kPa$ in 8.5 seconds nevertheless the gauge pressure can only rise to $28kPa$ in 13 seconds in the comparative group. That is, the self-sealing design can increase the gauge pressure and reduce the evacuation time.

Table II demonstrates that the DEC-cup and the Conv-cup perched on the wall successfully nine and eight times in ten trials in the absence of the crosswind respectively. However, the Conv-cup only succeeded two times under the crosswind disturbance and the DEC-cup still succeeded nine times in ten trials. The results indicate the performance of the Conv-cup decreased significantly under the crosswind. There are two cases for the failure of the Conv-cup. One is that the angular error is so large that the reaction force F_N is not enough to complete the sealing phase. Furthermore, the angular error becomes more common when two cups are used in our experiments, which also makes the perching more difficult (Fig.8 (b)). For the other case, although F_N is large enough induced by the impact of the quadrotor, there is no enough time to generate enough adhesion force to prevent the bounce of the quadrotor caused by F_N. For the DEC-cup, it can adapt larger angular error on the one hand and on the other hand the τ_g in (1) can correct the angular error of the firm cup and the F_g in (2) can also increase F_N. All these effects drastically avoid the first case as is show in Fig.8 (c). For the second case, the rebound velocity will be alleviated by F_g, which may pull the quadrotor back on the wall. The course of the perching using two kinds of cups can be seen in the submitted video.

For aerial gasping, Table II presents that the Conv-cup grasped the object zero time whereas the DEC-cup grasped nine times in ten trials. The key reason for the failure of the Conv-cup is that there is no enough F_N to seal the Conv-cup and a larger F_N may push the object away as shown in Fig.9 (b). For the DEC-cup, the smaller F_n is enough to seal the soft cup and the firm cup can also be sealed with the help of the soft cup. In this article, the experiments under crosswind were not conducted anymore because the difference between the two cups in the experiments without disturbance has been already significant. We have also submitted the video of these experiments.

Although the above effectiveness and advantages of the DEC-cup make the perching and aerial grasping more robust, a few failures still happened. The failure in the experiments of perching without crosswind was caused by the large swing of the multicopter, which prevented the adhesion of the firm cup. The failure in the experiments under crosswind was caused by the strong rebound which breaks free of the pull from the soft cup. In the experiments of aerial grasping, the grasping failed because the position errors were too large that the soft cup did not contact the object surface. The three different reasons leading to failures demonstrate that the occasional larger errors induced by the disturbance or inaccurate control may still exceed the adaptability of the DEC-cup.

V. CONCLUSION

We have presented a dual elasticity combined suction cup and an aerial manipulation system based on it to execute the perching or aerial grasping task. The combined cup has high adaptability to the angular error caused by multicopter and can also guarantee a larger adhesion force and a stiff base for subsequent manipulation. The relative axial position of the soft cup is optimized to maximal its contribution for the sealing of the firm cup. A novel self-sealing structure in the firm cup to reduce the air evacuation time is verified. The aerial manipulation system equipped with the combined cup is validated with the comparative flight experiments including perching on a wall and grasping an object. In these experiments, our design successfully perched in 9/10 trails under the crosswind disturbance and grasped the object in 9/10 trials without artificial disturbance. That is significantly larger than 2/10 or 0/10 in the conventional cup. These results

demonstrate that our design is more promising under the disturbance outdoors.

In future work, the equations (4-7) will be tested experimentally and be used to optimize the parameters of the self-sealing mechanism. Secondly, other spatial configurations of the soft cup and the firm cup will be researched. Finally, the autonomous perching and aerial grasping relying on the onboard sensors as well as the perch-and-manipulate applications based on our DEC-cup will also be studied.

ACKNOWLEDGMENT

The authors appreciate the professional help from Prof. Feifei Chen from Shanghai Jiaotong University.

REFERENCES

[1] H. Paul, K. Ono, R. Ladig, and K. Shimonomura, *A multirotor platform employing a three-axis vertical articulated robotic arm for aerial manipulation tasks*, 2018, pp. 478–485.

[2] A. Ollero, G. Heredia, A. Franchi, G. Antonelli, K. Kondak, A. Sanfeliu, A. Viguria, J. R. Martinez-de Dios, F. Pierri, J. Cortés *et al.*, "The aeroarms project: Aerial robots with advanced manipulation capabilities for inspection and maintenance," *IEEE Robotics & Automation Magazine*, vol. 25, no. 4, pp. 12–23, 2018.

[3] M. Á. Trujillo, J. R. Martínez-de Dios, C. Martín, A. Viguria, and A. Ollero, "Novel aerial manipulator for accurate and robust industrial ndt contact inspection: A new tool for the oil and gas inspection industry," *Sensors*, vol. 19, no. 6, p. 1305, 2019.

[4] U. A. Fiaz, M. Abdelkader, and J. S. Shamma, "An intelligent gripper design for autonomous aerial transport with passive magnetic grasping and dual-impulsive release," in *2018 IEEE/ASME International Conference on Advanced Intelligent Mechatronics (AIM)*. IEEE, 2018, pp. 1027–1032.

[5] H. Lee and H. J. Kim, "Estimation, control, and planning for autonomous aerial transportation," *IEEE Transactions on Industrial Electronics*, vol. 64, no. 4, pp. 3369–3379, 2016.

[6] P. Ramon Soria, B. C. Arrue, and A. Ollero, "Detection, location and grasping objects using a stereo sensor on uav in outdoor environments," *Sensors*, vol. 17, no. 1, p. 103, 2017.

[7] A. Suarez, G. Heredia, and A. Ollero, "Compliant and lightweight anthropomorphic finger module for aerial manipulation and grasping," in *Robot 2015: Second Iberian Robotics Conference*. Springer, 2016, pp. 543–555.

[8] H. Tsukagoshi, M. Watanabe, T. Hamada, D. Ashlih, and R. Iizuka, "Aerial manipulator with perching and door-opening capability," in *2015 IEEE International Conference on Robotics and Automation (ICRA)*. IEEE, 2015, pp. 4663–4668.

[9] M. A. Estrada, S. Mintchev, D. L. Christensen, M. R. Cutkosky, and D. Floreano, "Forceful manipulation with micro air vehicles," *Science Robotics*, vol. 3, no. 23, p. eaau6903, 2018.

[10] H. Zhang, J. Sun, and J. Zhao, "Compliant bistable gripper for aerial perching and grasping," in *2019 International Conference on Robotics and Automation (ICRA)*. IEEE, 2019, pp. 1248–1253.

[11] C. Luo, L. Yu, and P. Ren, "A vision-aided approach to perching a bioinspired unmanned aerial vehicle," *IEEE Transactions on Industrial Electronics*, vol. 65, no. 5, pp. 3976–3984, 2017.

[12] T.-J. Lin, S. Long, and K. A. Stol, "Automated perching of a multirotor uav atop round timber posts," in *2018 IEEE/ASME International Conference on Advanced Intelligent Mechatronics (AIM)*. IEEE, 2018, pp. 486–491.

[13] J. Qi, J. Kang, and X. Lu, "Design of autonomous indoor aerial manipulator," in *2018 13th World Congress on Intelligent Control and Automation (WCICA)*. IEEE, 2018, pp. 263–268.

[14] M. Tieu, D. M. Michael, J. B. Pflueger, M. S. Sethi, K. N. Shimazu, T. M. Anthony, and C. L. Lee, *Demonstrations of bio-inspired perching landing gear for UAVs*, 2016, vol. 9797, p. 97970X.

[15] J. Thomas, G. Loianno, K. Daniilidis, and V. Kumar, "Visual servoing of quadrotors for perching by hanging from cylindrical objects," *IEEE robotics and automation letters*, vol. 1, no. 1, pp. 57–64, 2015.

[16] M. Kovač, J. Germann, C. Hürzeler, R. Y. Siegwart, and D. Floreano, "A perching mechanism for micro aerial vehicles," *Journal of Micro-Nano Mechatronics*, vol. 5, no. 3-4, pp. 77–91, 2009.

[17] M. T. Pope, C. W. Kimes, H. Jiang, E. W. Hawkes, M. A. Estrada, C. F. Kerst, W. R. Roderick, A. K. Han, D. L. Christensen, and M. R. Cutkosky, "A multimodal robot for perching and climbing on vertical outdoor surfaces," *IEEE Transactions on Robotics*, vol. 33, no. 1, pp. 38–48, 2016.

[18] D. Mellinger, M. Shomin, and V. Kumar, "Control of quadrotors for robust perching and landing," in *Proceedings of the International Powered Lift Conference*, 2010, pp. 205–225.

[19] Y. Liu, G. Sun, and H. Chen, "Impedance control of a bio-inspired flying and adhesion robot," in *2014 IEEE International Conference on Robotics and Automation (ICRA)*. IEEE, 2014, pp. 3564–3569.

[20] H. W. Wopereis, T. Van Der Molen, T. Post, S. Stramigioli, and M. Fumagalli, "Mechanism for perching on smooth surfaces using aerial impacts," in *2016 IEEE International Symposium on Safety, Security, and Rescue Robotics (SSRR)*. IEEE, 2016, pp. 154–159.

[21] A. Kalantari, K. Mahajan, D. Ruffatto, and M. Spenko, "Autonomous perching and take-off on vertical walls for a quadrotor micro air vehicle," in *2015 IEEE International Conference on Robotics and Automation (ICRA)*. IEEE, 2015, pp. 4669–4674.

[22] M. Graule, P. Chirarattananon, S. Fuller, N. Jafferis, K. Ma, M. Spenko, R. Kornbluh, and R. Wood, "Perching and takeoff of a robotic insect on overhangs using switchable electrostatic adhesion," *Science*, vol. 352, no. 6288, pp. 978–982, 2016.

[23] K. Zhang, P. Chermprayong, T. Alhinai, R. Siddall, and M. Kovac, "Spidermav: Perching and stabilizing micro aerial vehicles with bio-inspired tensile anchoring systems," in *2017 IEEE/RSJ International Conference on Intelligent Robots and Systems (IROS)*. IEEE, 2017, pp. 6849–6854.

[24] G. Loianno, V. Spurny, J. Thomas, T. Baca, D. Thakur, D. Hert, R. Penicka, T. Krajnik, A. Zhou, A. Cho *et al.*, "Localization, grasping, and transportation of magnetic objects by a team of mavs in challenging desert-like environments," *IEEE Robotics and Automation Letters*, vol. 3, no. 3, pp. 1576–1583, 2018.

[25] R. A. Mattar and R. Kalai, "Development of a wall-sticking drone for non-destructive ultrasonic and corrosion testing," *Drones*, vol. 2, no. 1, p. 8, 2018.

[26] Y. Guo, J. Zhang, Y. Ju, and X. Guo, "Climbing reconnaissance drone design," vol. 452, no. 4, p. 042060, 2018.

[27] W. R. Roderick, M. R. Cutkosky, and D. Lentink, "Touchdown to take-off: at the interface of flight and surface locomotion," *Interface focus*, vol. 7, no. 1, p. 20160094, 2017.

[28] S. Sareh, R. Siddall, T. Alhinai, and M. Kovac, *Bio-inspired soft aerial robots: adaptive morphology for high-performance flight*. Springer, 2017.

[29] S. Du, H. Chen, Y. Liu, and R. Hu, "Unified switching between active flying and perching of a bioinspired robot using impedance control," *Journal of Robotics*, vol. 2015, 2015.

[30] X. Ye, Y. Liu, W. Li, and J. Fan, "Control design for ceiling-perching flying robot with dynamic feedforward compensation," in *2017 IEEE 7th Annual International Conference on CYBER Technology in Automation, Control, and Intelligent Systems (CYBER)*. IEEE, 2017, pp. 852–857.

[31] X. Liu, Y. He, B. Chen, Y. Hou, K. Bi, and D. Li, "A vision-based unmanned aircraft system for autonomous grasp & transport," in *2019 International Conference on Unmanned Aircraft Systems (ICUAS)*. IEEE, 2019, pp. 1186–1193.

[32] C. C. Kessens and J. P. Desai, "Design, fabrication, and implementation of self-sealing suction cup arrays for grasping," in *2010 IEEE International Conference on Robotics and Automation*. IEEE, 2010, pp. 765–770.

[33] C. C. Kessens, J. Thomas, J. P. Desai, and V. Kumar, "Versatile aerial grasping using self-sealing suction," in *2016 IEEE international conference on robotics and automation (ICRA)*. IEEE, 2016, pp. 3249–3254.

[34] C. C. Kessens, M. Horowitz, C. Liu, J. Dotterweich, M. Yim, and H. L. Edge, "Toward lateral aerial grasping & manipulation using scalable suction," in *2019 International Conference on Robotics and Automation (ICRA)*. IEEE, 2019, pp. 4181–4186.

[35] C. C. Kessens and J. P. Desai, "Versatile passive grasping for manipulation," *IEEE/ASME Transactions on Mechatronics*, vol. 21, no. 3, pp. 1293–1302, 2016.

[36] B. Bahr, Y. Li, and M. Najafi, "Design and suction cup analysis of a wall climbing robot," *Computers & electrical engineering*, vol. 22, no. 3, pp. 193–209, 1996.